SEMARAK ILMU PUBLISHING

Semarak Engineering Journal

Journal homepage:
https://semarakilmu.com
ISSN: 3036-0145



Numerical Simulation of Graphene-Nanoplatelet Nanofluid Convection in a Microtube Automotive Radiator

Leslie Toh Kok Lik[1], Ting Tiew Wei[1,2,*]

[1] School of Engineering and Technology, University of Technology Sarawak, 96000 Sibu, Sarawak, Malaysia

[2] Centre for Research of Innovation and Sustainable Development, University of Technology Sarawak, 96000 Sibu, Sarawak, Malaysia

ARTICLE INFO

Article history:
Received 29 January 2026
Received in revised form 8 March 2026
Accepted 13 March 2026
Available online 3 April 2026

Keywords:

Graphene nanoplatelet; heat transfer enhancement; nanofluid; radiator

ABSTRACT

This study investigates the convection performance of graphene nanoplatelets (GnP) in water-based nanofluid for microtube automotive radiators, with a focus on the impact of GnP concentration, nanoparticle size, and temperature on the thermophysical properties and heat transfer behavior. The results indicate that increasing GnP concentration raises the density but reduces the specific heat capacity of the nanofluid. Thermal conductivity improves with both higher GnP concentration and temperature, outperforming the basefluid by 667%. Conversely, viscosity increases with increasing GnP concentration but decreases with rising temperature. Using ANSYS Fluent, the study simulates the thermal performance of the microtube radiator and finds that at Reynolds numbers below 100, the average Nusselt number improves with both GnP concentration and Reynolds number, by as much as 1063%. However, above a Reynolds number of 100, the thermal performance deteriorates due to viscous dissipation. The study further reveals that reducing the inlet temperature increases the Nusselt number at high Reynolds numbers, while at low Reynolds numbers, both basefluid and GnP-water nanofluid show an enhancement in heat transfer. A decrease in nanoparticle thickness also enhances the Nusselt number when viscous dissipation is significant. The results suggest that the basefluid is more effective at high Reynolds numbers in a microtube automotive radiator, whereas the GnP-water nanofluid is better suited for low Reynolds number flows.

1. Introduction

The escalating global demand for energy resources has emerged as a critical challenge [1], particularly in the transportation sector, which heavily relies on gasoline- and diesel-fueled vehicles for rural and urban mobility [2]. As reported by World Energy Council, the transportation sector accounts for over 60% of global oil consumption, approximately fifty-one million barrels per day [3]. Projections from the U.S. Energy Information Administration indicate that this figure will rise to nearly seventy million barrels per day by 2040 [4]. Furthermore, the automotive sector contributes approximately 20% of global greenhouse gas emissions [5], making it a significant source of air

* *Corresponding author.*
E-mail address: tiewwei@gmail.com

pollution [2]. These environmental and energy concerns have intensified efforts to develop advanced technologies for higher-efficiency vehicles. Improving fuel economy has become a key objective for automotive manufacturers, necessitating the design of engines with enhanced thermal and energy efficiency [1, 6]. However, limitations such as engine overheating hinder optimal engine performance, underscoring the critical importance of effective thermal management systems. Enhancing the convective heat transfer performance of automotive radiators is a vital step toward addressing these limitations and improving overall engine efficiency in modern vehicles [7].

One of the primary constraints on radiator performance lies in the low thermal conductivity of conventional coolants, which restricts their ability to dissipate heat effectively. To address this issue, innovative approaches have been developed, including the use of engineered colloidal fluids known as nanofluids [7, 8]. These fluids consist of nanoparticles, typically less than 100 nm in diameter, suspended within a traditional coolant base. Nanofluids exhibit enhanced heat transfer properties due to their high specific surface area, which significantly improves thermal exchange efficiency [9-13]. Additionally, the nanoscale size of the particles prevents clogging in macro- and milli-sized channels, making them particularly suitable for integration into automotive cooling systems [14]. As such, nanofluids represent a promising avenue for enhancing the thermal performance of radiators and addressing the increasing demand for energy-efficient and environmentally sustainable automotive technologies.

The high thermal conductivity of metallic particles has prompted extensive research into the utilization of metal-based nanoparticles to enhance heat transfer performance in automotive radiators [15, 16]. However, carbon-based nanoparticles, such as graphene—comprising a single layer of pure carbon—possess significantly higher thermal conductivities compared to metal nanoparticles [17, 18]. This superior property has positioned graphene-based nanoparticles as a promising alternative for further improving the cooling efficiency of automotive radiators. Notably, most studies to date have focused on the suspension of graphene nanoplatelets (GnP) in ethylene glycol (EG)/water mixtures as the basefluid for automotive cooling systems [10, 19-21]. The suspension of GnP in EG/water basefluid has been shown to enhance the radiator's heat transfer rate by 68% [19] and improve the convective heat transfer coefficient by 58% [10], as reported in experimental studies. A similar result was observed for a hybrid nanofluid comprising GnP and cellulose nanocrystals, which resulted in a 51.9% increase in the convective heat transfer coefficient of automotive radiator cooling systems [20]. Additionally, Ponangi et al. [21] examined the effects of carboxyl graphene and graphene oxide suspended in EG/water. Their study revealed an increase in the radiator's Nusselt number by up to 11 times, highlighting the potential of these nanofluids as highly effective coolants for automotive radiators. Research on the convective performance of water-based GnP nanofluids in radiators for enhancing automotive engine cooling is limited. Toh et al. [22] conducted a comprehensive numerical study to examine the convective performance of GnP suspensions in water within millimeter-sized automotive radiators. Their findings revealed a substantial enhancement in the Nusselt number, with an increase of up to 1816%, when the aspect ratios of the particles and tube were reduced [22]. Furthermore, the study identified a hydraulic diameter threshold near 1 mm, below which GnP-water nanofluid negatively impacted the radiator's thermal performance, suggesting the need for further investigation into this phenomenon [22].

The detrimental effect of nanoparticles on heat transfer performance, attributed to the existence of a tube aspect ratio threshold within the micrometer range, has also been reported by Ting et al. [23]. The presence of the threshold aspect ratio is attributed to the balance between two opposing mechanisms. A reduction in the aspect ratio increases viscous dissipation, which degrades the heat transfer coefficient. In contrast, an increase in nanoparticle concentration enhances the effective thermal conductivity of the nanofluid, thereby improving convective heat transfer. When the aspect

ratio falls below the threshold, the adverse impact of increased viscous dissipation surpasses the beneficial effect of enhanced thermal conductivity. This results in a negative effect of nanoparticles on heat transfer performance in microchannels [23]. Fani et al. [24] analyzed Brownian motion and viscous dissipation in microchannel heat sinks with CuO-water nanofluid. Thermal performance improved with higher inlet temperatures and CuO loadings due to increased Brownian motion. However, viscous dissipation reduced the average Nusselt number by up to 4.3%. Nimmagadda et al. [25] analyzed heat transfer performance in microchannels utilizing hybrid nanofluids under laminar flow conditions. The study demonstrated that the convective heat transfer coefficient increased with both Reynolds number and nanoparticle loading, achieving an enhancement of 148.62% when compared to the base fluid. Akhai et al. [26] investigated the use of CuO nanofluid as a cooling medium in rectangular microchannel radiators for vehicles, reporting a 40% enhancement in thermal conductivity and a 116% improvement in the heat transfer coefficient compared to water. These findings highlight the potential of CuO nanofluid as an effective alternative to conventional cooling fluids in automotive radiator applications. While nanofluids demonstrate considerable promise in enhancing heat transfer performance in microscale devices, their efficiency is significantly influenced by factors such as nanoparticle concentration, Reynolds number, and channel geometry [23-25]. However, viscous dissipation, particularly at elevated Reynolds numbers and nanoparticle concentrations, has been observed to reduce heat transfer performance performance [23, 24]. Further research is necessary to evaluate the thermal performance of microtube radiators incorporating nanofluids and to develop optimization strategies for improving their thermal efficiency.

Recent literature on graphene-based nanofluid flow in automotive radiators primarily utilizes mixtures of water and ethylene glycol (EG) as base fluids, typically within macro- or milli-scale channels [19-21, 27]. Despite extensive research into the heat transfer characteristics of nanofluids, the convective performance of Graphene-Nanoplatelet (GnP) fluids within microtube-based automotive radiators remains insufficiently understood. Due to the increased viscous dissipation caused by the reduction in radiator diameter to the microscale and the presence of nanoparticle suspension, the thermal performance of microtube radiators with nanofluid flow can differ significantly. Ajuka et al. [28] investigated the entropy generation characteristics of GnP nanofluid in micro- and mini-channels for automotive cooling applications. Their findings indicated that increasing the GnP volume fraction in the base fluid reduced the entropy generation ratio, highlighting the beneficial impact of the nanofluid's enhanced thermal properties from the second law of thermodynamics. However, from the perspective of the first law of thermodynamics, no numerical studies explicitly examine the convective performance of water-based GnP nanofluids in microtube radiators for automotive cooling. Current literature, such as the work by Toh et al. [22], indicates a performance threshold where heat transfer enhancement in millimeter-sized radiators transitions to potential deterioration as hydraulic diameters drop below 1 mm. The underlying physics of this microscale behavior, specifically the impact of viscous dissipation coupled with varying nanoparticle concentrations and sizes, remains an unaddressed gap. This study aims to fill this void by providing a systematic numerical investigation into the heat transfer potential and fluid dynamics of GnP nanofluids in compact, microscale radiator systems. The effects of key parameters, including Reynolds number, inlet temperature, nanoparticle thickness, and tube diameter, on the heat transfer performance of the microtube radiator are systematically analyzed. Additionally, temperature contours of the nanofluid flow are analyzed to deepen the understanding of the physical mechanisms underlying performance enhancement in microtube automotive radiators utilizing graphene-based nanoparticles suspended in water.

2. Methodology

A typical automotive radiator is composed of numerous tubes paired with plate fins, enabling cooling through heat transfer between the coolant fluid and surrounding air. In this study, ANSYS Fluent is employed to simulate the heat transfer performance of a radiator tube at the micrometer scale using GnP suspension. Figure 1 provides a cross-sectional view of the microtube radiator setup in ANSYS, where a quarter of the microtube cross-section is modeled, applying a symmetry boundary condition to reduce mesh size. The hydraulic diameter of the microtube is D = 200 µm and the tube length is L = 21.85 mm.

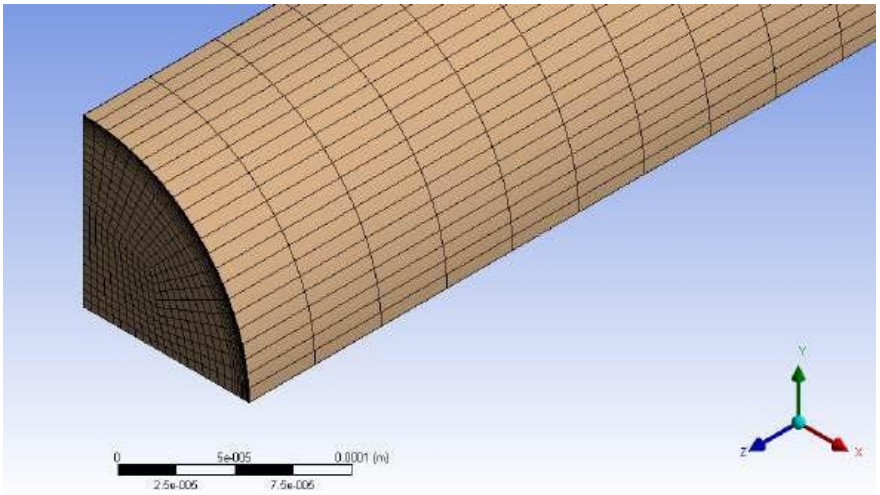


Fig. 1. Geometry and meshing layout for a radiator microtube

The GnP-based nanofluid within the radiator tube is assumed to exhibit incompressible flow under laminar conditions, with negligible radiation heat transfer effects. Graphene nanoplatelets were selected for this investigation due to their planar structure, which offers superior thermal conductivity and a higher surface-area-to-volume ratio compared to traditional metal-oxide nanoparticles. Furthermore, this study builds upon our previous findings [22], which highlighted a transition in convective performance as radiator scales move from the millimeter to the micrometer range. By utilizing the same GnP suspension, this work provides a direct comparative analysis to determine if the microscale performance degradation observed in earlier studies persists under varying concentrations and viscous dissipation effects. Due to the low nanoparticle concentration, a single-phase fluid approach is adopted, allowing the nanofluid to behave similarly to basefluid [22]. Based on these assumptions, the governing equations for continuity, momentum, and energy are solved in ANSYS Fluent within a 3-dimensional flow field. The continuity equation is expressed as [29]

$$(\nabla \cdot V) = 0 \tag{1}$$

The momentum equation can be written as [29]

$$\rho(\nabla \cdot V)V = -\nabla P + \mu \nabla^2 V \tag{2}$$

The energy equation can be defined as [29]

$$\rho C_p(\nabla \cdot V)T = k\nabla^2 T + \mu\Phi \tag{3}$$

where P represents pressure, T is temperature and Φ represents the viscous dissipation function.

2.1 Thermophysical Properties Correlations

In this study, the thermophysical properties of GnP-based nanofluids are estimated using a mathematical approach. The density, specific heat capacity, thermal conductivity, and viscosity of the nanofluids are determined under the assumption that nanoparticles are uniformly dispersed in the basefluid at a constant concentration [30]. Using a volume-averaging method, the density of the nanofluid is calculated as [31]

$$\rho_{nf} = \phi\rho_p + (1 - \phi)\rho_{bf} \tag{4}$$

The specific heat capacity can be calculated as [32]

$$C_{p,nf} = \frac{\phi\rho_p C_{pp} + (1 - \phi)\rho_{bf} C_{pbf}}{\rho_{nf}} \tag{5}$$

where ρ is density, C_p represents specific heat capacity, ϕ is defined as volumetric concentration, subscript "*bf*" represents basefluid, subscript "*nf*" indicates nanofluid and subscript "*p*" represents nanoparticle. These two equations are commonly used to determine the density and the specific heat capacity of nanofluids [33, 34]. The viscosity of GnP-based nanofluid can be expressed as [22]

$$\mu_{nf} = C_\mu \mu_{bf} \tag{6}$$

$$C_\mu = (1+\sigma^{1.675}\phi) \tag{7}$$

where μ is dynamic viscosity, C_μ is viscosity coefficient of GnP-based nanofluid and $\sigma = \{0.312\beta/[\ln(2\beta - 1.5)]\} + 2 - \{0.5/[\ln(2\beta - 1.5)]\} - (1.872/\beta)$ is intrinsic viscosity and $\beta = D_p / t_p$ is axis ratio. As reported by Toh et al. [22], the current viscosity correlation aligns well with existing literature [35-37], with error margins ranging from 0.00778% to 5.57%. The thermal conductivity of GnP-based nanofluids is determined using Nan's model [38]

$$k_{nf} = C_k k_{bf} \tag{8}$$

$$C_k = \frac{3 + \phi[2\gamma_{11}(1 - \ell_{11}) + \gamma_{33}(1 - \ell_{33})]}{3 - \phi(2\gamma_{11}\ell_{11} + \gamma_{33}\ell_{33})} \tag{9}$$

where C_k is constant coefficient of thermal conductivity for GnP-based nanofluid and k represents thermal conductivity. ℓ_{11} and ℓ_{33} are geometrical factors which can be defined by

$$\ell_{11} = \frac{\xi_p^2}{2(\xi_p^2 - 1)} + \frac{\xi_p}{2(1 - \xi_p^2)^{3/2}}\cos^{-1}\xi_p \quad \text{for} \quad \xi_p < 1 \tag{10}$$

$$\ell_{33} = 1 - 2\ell_{11} \tag{11}$$

ξ_p represents the nanoparticle aspect ratio which can be expressed as

$$\xi_p = \frac{t_p}{D_p} \tag{12}$$

where t_p is particle thickness and D_p represents particle diameter. γ_{11} and γ_{33} can be expressed as

$$\gamma_{11} = \frac{k_{11} - k_{bf}}{k_{bf} + \ell_{11}(k_{11} - k_{bf})} \tag{13}$$

$$\gamma_{33} = \frac{k_{33} - k_{bf}}{k_{bf} + \ell_{33}(k_{33} - k_{bf})} \tag{14}$$

In Eq. (13) and Eq. (14), k_{11} and k_{33} represent the equivalent thermal conductivities along the *x*-axis and *z*-axis and can be defined as

$$k_{11} = \frac{k_{par}}{1 + \delta \ell_{11} k_{par} / k_{bf}} \tag{15}$$

$$k_{33} = \frac{k_{per}}{1 + \delta \ell_{33} k_{per} / k_{bf}} \tag{16}$$

where k_{par} is particle thermal conductivity in parallel to surface and k_{per} is particle thermal conductivity in perpendicular to surface. δ is a dimensionless parameter which is expressed as

$$\delta = (1 + 2\xi_p)\frac{2K_r}{t_p} \quad \text{for} \quad \xi_p < 1 \tag{17}$$

where K_r represents Kapitza radius which can be defined as

$$K_r = R_i k_{bf} \tag{18}$$

Based on Eq. (18), R_i represents interfacial thermal resistance which can be written as

$$R_i = \frac{t_i}{k_i} \tag{19}$$

with t_i as the thickness of interfacial boundary layer and k_i represents thermal conductivity of interfacial boundary layer. The current thermal conductivity model predicts the thermal conductivity of GnP-based nanofluids with a satisfactory accuracy, demonstrating a percentage error of 2.29% [22].

2.2 Boundary Conditions

ANSYS Fluent is employed to analyze the thermal performance of GnP-based nanofluid in a radiator microtube. The simulation is conducted using double precision, a second-order upwind scheme, an energy model, and viscous heating, with all results computed to a convergence criterion of 10^{-6}. The velocity components, temperature, and pressure are solved within the tube's internal computational domain. For data post-processing, the wall temperature, wall heat flux, and bulk mean temperature are recorded for the calculations of heat transfer coefficient and Nusselt number. As illustrated in Figure 2, uniform axial inlet velocity and pressure outlet boundary conditions are applied to approximate the actual flow pattern [6], while the convective heat transfer coefficient and wall temperature for the tube are set to h_o = 50 W/m^{2}K and T_o = 303 K, representing conditions equivalent to an automotive vehicle moving at a speed of 72 km/h [39]. To optimize meshing, a symmetry boundary condition is implemented as illustrated in Figure 1 and Figure 2, and a no-slip boundary condition is applied at the wall. This investigation is conducted in the laminar flow regime, with Reynolds number determined by the inlet velocity. Temperature-dependent thermophysical properties of the GnP-based nanofluid, as defined by Eq. (4) to Eq. (19), are input into ANSYS Fluent.

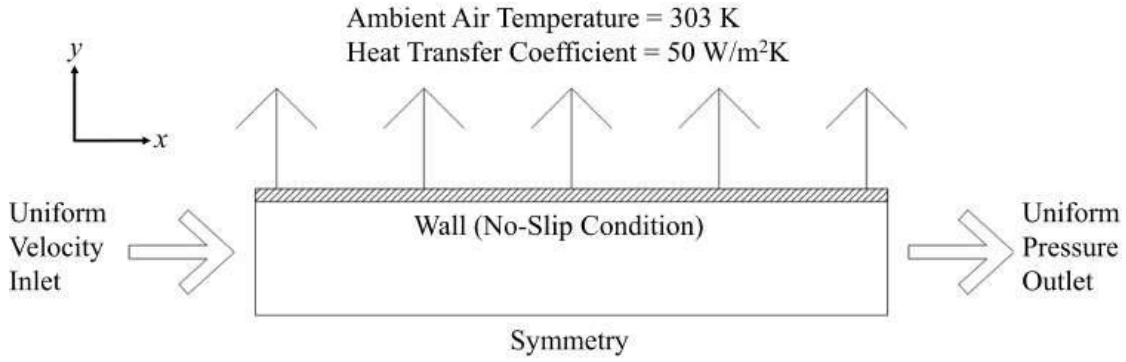


Fig.2. Boundary conditions of the microtube radiator

In the micrometer-sized tube, the nanofluid can be treated as a continuum by evaluating the Knudsen number [40], defined as the ratio of the nanofluid molecule mean free path to the geometry diameter, Kn = λ_{nf} / D [41]. According to Gad-el-Hak [41], the continuum approach is valid when the Knudsen number is below 0.1. Table 1 presents the Knudsen numbers from existing numerical studies on micrometer-sized geometries with carbon-based nanofluids. As shown in Table 1, when Kn ≤ 0.01, the continuum assumption and no-slip boundary condition are commonly applied [42-47]. Therefore, the governing equations of Eq. (1) to Eq. (3) are appropriate for numerical analysis in micrometer-sized tubes with nanoparticle suspensions when Kn ≤ 0.01. This study explores various parameters in microtube radiators with GnP suspensions, including volumetric concentration, Reynolds number, inlet temperature, particle thickness, and tube diameter.

Table 1
Knudsen number of the various numerical studies in micrometer-sized geometry

Nanoparticles	D_p	t_p	D	Kn	Slip Condition	Reference
GnP	2 µm	-	200 µm	0.01	No slip condition	[45]
GnP	2 µm	-	200 µm	0.01	No slip condition	[46]
GnP	2 µm	-	200 µm	0.01	No slip condition	[42]
MWCNT	25 nm	1, 3, 5 nm	42.68 µm	0.00058	No slip condition	[47]
SWCNT	2 nm	3 µm	200 µm	0.015	No slip condition	[44]
SWCNT	15 nm	30 µm	450 µm	0.067	No slip condition	[43]

2.3 Data Reduction

In the present study, Reynolds number of GnP-based nanofluid is defined as

$$\mathrm{Re} = \frac{\rho V D}{\mu} \tag{20}$$

where D represents diameter of the tube. The local heat transfer coefficient, h_l along the circumference of the tube can be calculated from

$$h_l = \frac{q''}{(T_w - T_b)} \tag{21}$$

By averaging local heat transfer coefficient over the perimeter of the tube, the average local heat transfer coefficient is defined as $\bar{h}_z = \sum h_l \ / \ n$ where n represents number of points. The average local Nusselt number, $\overline{Nu}_z$ along the tube length can be defined as

$$\overline{Nu}_z = \frac{\bar{h}_z D_h}{k_{bf}} \tag{22}$$

The average heat transfer coefficient, $\bar{h}$ and average Nusselt number, $\overline{Nu}$ over the entire tube length can be written, respectively, as

$$\bar{h} = \frac{1}{L}\int_0^L \bar{h}_z dz \tag{23}$$

$$\overline{Nu} = \frac{1}{L}\int_0^L \overline{Nu}_z dz \tag{24}$$

where L represents tube length. The percentage enhancement of the average Nusselt number, Δ can be defined as

$$\Delta = \frac{\overline{Nu}_{nf} - \overline{Nu}_{bf}}{\overline{Nu}_{bf}} \tag{25}$$

2.4 Validation

The validation of the present study is conducted by comparing the average local heat transfer coefficient, $\bar{h}_z$ along the tube length with the results of Vajjha et al. [6], using a coolant mixture of 40% water and 60% ethylene glycol at Re = 2000, as shown in Figure 3. The results demonstrate good agreement between the two studies, with a maximum error of 4.64%. These findings provide strong validation for the accuracy of the modeling approach used in this study.

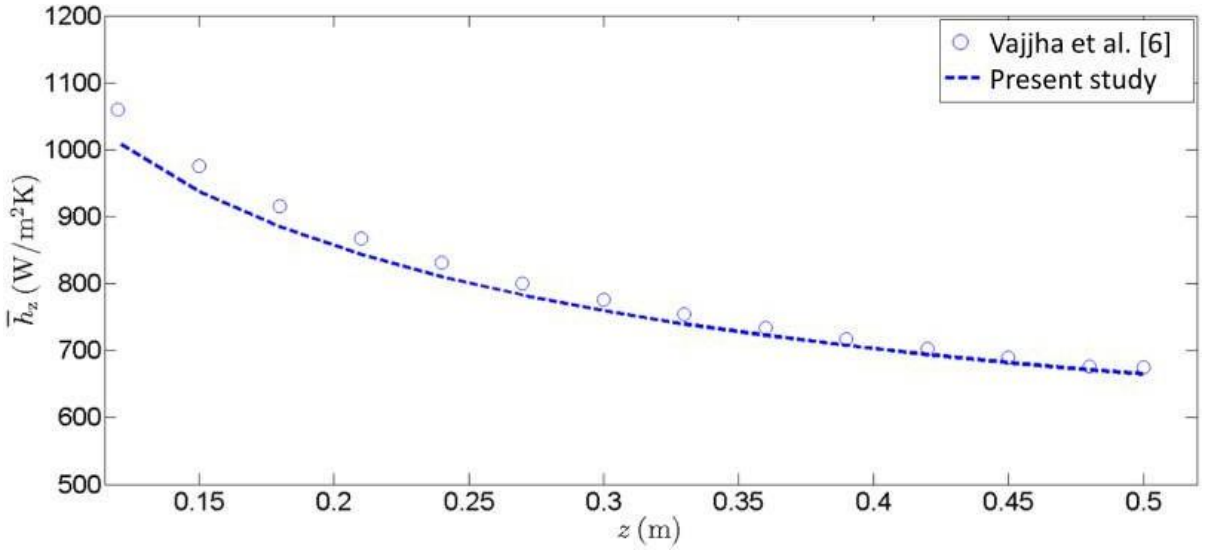


Fig.3. Comparison of the local heat transfer coefficient of present study with Vajjha *et al.* [6]

3. Result and Discussion

3.1 Thermophysical Properties of Nanofluid

The thermophysical properties of a GnP-based nanofluid, with water as the basefluid, were determined to assess the thermal performance of a microtube radiator. The GnP nanoparticles are characterized by t_p = 2nm and D_p = 2 µm. The thermophysical properties were calculated using Eq. (4) to Eq. (19). Table 2 presents the thermophysical properties of the GnP nanoparticles, while the thermophysical properties of water were obtained from Bergman et al. [48].

Table 2
Thermophysical properties of GnP nanoparticles

Property	Thermophysical properties for GnP nanoparticles	Reference
ρ	2200 kg/m^3	[17]
C_p	643 J/kgK	[49]
k_{par}	3000 W/mK	[17]
k_{pen}	6 W/mK	[17]

Figure 4 illustrates the density of the GnP-water nanofluid with t_p = 2nm and D_p = 2 µm. The density of the GnP-water nanofluid increases as ϕ rises, attributed to the higher density of GnP nanoparticles relative to the basefluid. Besides, the density of the nanofluid reduces with the reduction of the temperature due to the reduction of the density of basefluid at higher temperature. The density of GnP-water nanofluid with ϕ = 1.0% increases marginally by 1.24% at 333 K compared to the basefluid.

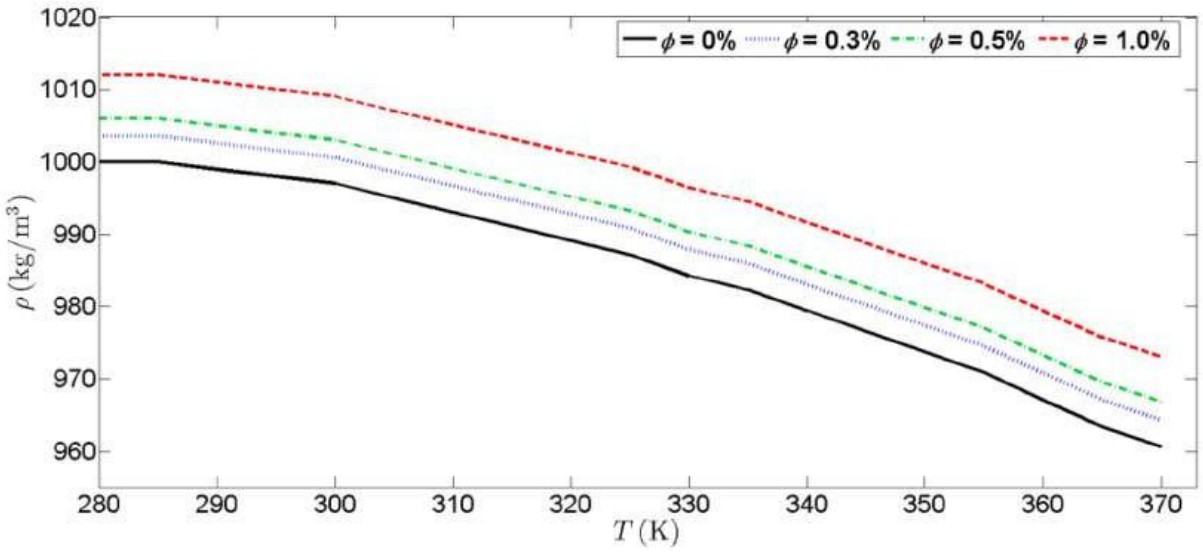


Fig.4. Density of GnP-water nanofluid with respect to temperature for various ϕ

Figure 5 presents the specific heat capacity of the GnP-water nanofluid with the variations of ϕ. The specific heat capacity of the GnP-water nanofluid decreases with increasing GnP concentration, due to the lower specific heat capacity of GnP nanoparticles compared to the basefluid. Furthermore, the specific heat capacity of the GnP-water nanofluid varies with temperature, reflecting the properties of the basefluid. At 333 K, the specific heat capacity of GnP-water nanofluid with ϕ = 1.0% is reduced by 1.87% relative to the basefluid. However, the reduction in specific heat capacity remains minimal with the increases of GnP nanoparticle loading.

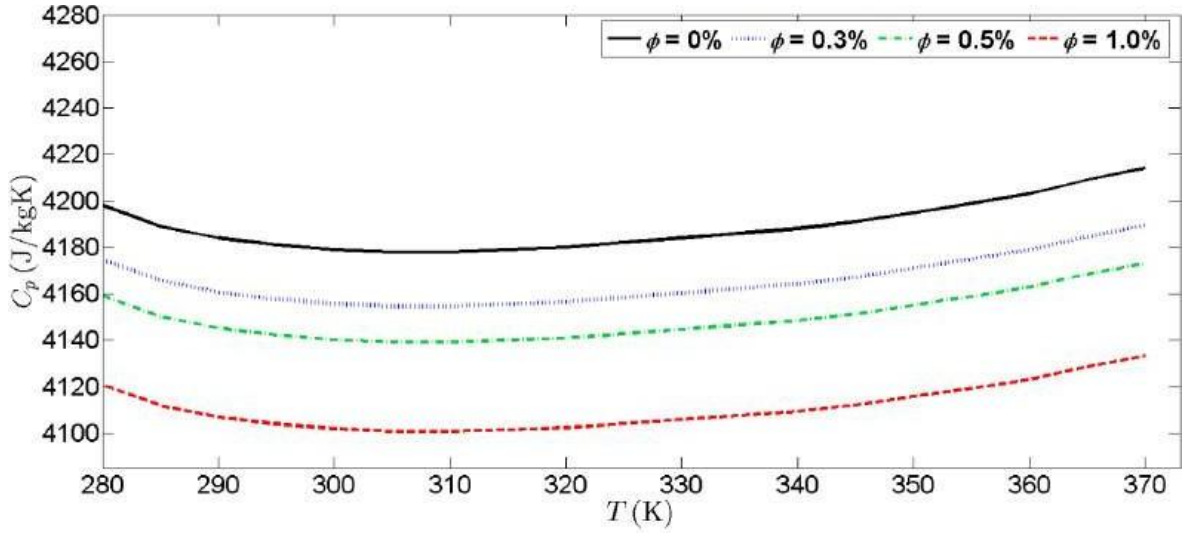


Fig.5. Specific heat capacity of GnP-water nanofluid with respect to temperature for various ϕ

According to Nan et al. [38], the enhancement in thermal conductivity of GnP-water nanofluid is significantly influenced by interfacial thermal resistance. In this study, a perfect interface assumption is applied, with a Kapitza radius set to zero [38, 50]. Figure 6 shows the thermal conductivity of GnP-water nanofluid for various ϕ. The thermal conductivity of the nanofluid varies with ϕ and temperature, increasing with higher ϕ and elevated temperatures due to factors such as Brownian motion, nanoparticle clustering, liquid layering, and micro-convection effects [10, 27, 51, 52]. The high thermal conductivity of GnP nanoparticles, compared to the basefluid, further contributes to

this enhancement. At 333 K, the thermal conductivity of ϕ = 1.0% GnP-water nanofluid improves by 667.16% relative to the basefluid, i.e. the thermal conductivity increased from 0.65 W/m·K for pure water to 4.99 W/m·K for the nanofluid. Additionally, when compared to GnP-water nanofluid with t_p = 10 nm and D_p = 2 µm at 333 K [22], the thermal conductivity for ϕ = 1.0% GnP-water nanofluid with t_p = 2 nm and D_p = 2 µm is 192.75% higher. This thermal conductivity enhancement has the potential to optimize the radiator's thermal performance, with higher thermal conductivity further improving overall efficiency [35].

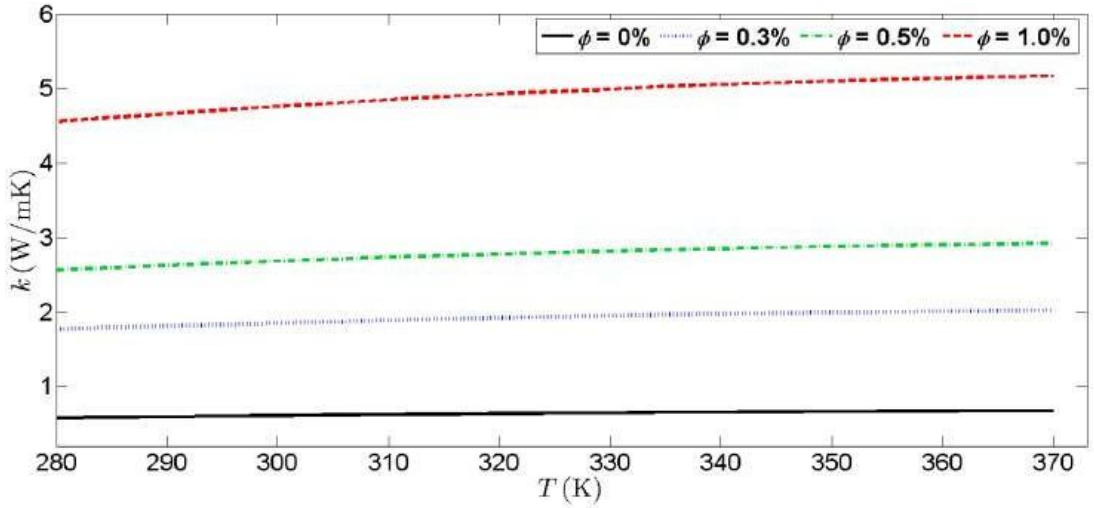


Fig.6. Thermal conductivity of GnP-water nanofluid with respect to temperature for various ϕ

Figure 7 presents the viscosity of the GnP-water nanofluid with different ϕ. The viscosity of the GnP-water nanofluid varies with particle size, as described by Eq. (6) and Eq. (7). It increases with higher ϕ and decreases as temperature rises, attributed to reduced intermolecular interactions at elevated temperatures, which results in lower viscosity [35]. At 333 K, the viscosity of the GnP-water nanofluid with ϕ = 1.0% is 774.34% greater than that of the basefluid. Based on Figure 7, the viscosity for GnP-water nanofluid with t_p = 2 nm and D_p = 2 µm is 333.91% higher than that of the nanofluid with t_p = 10 nm and D_p = 2 µm [22]. This elevated viscosity could intensify viscous dissipation effects within a microtube radiator. Unless otherwise specified, all thermal performance assessments for the microtube radiator radiator are based on the properties depicted in Figure 4 to Figure 7.

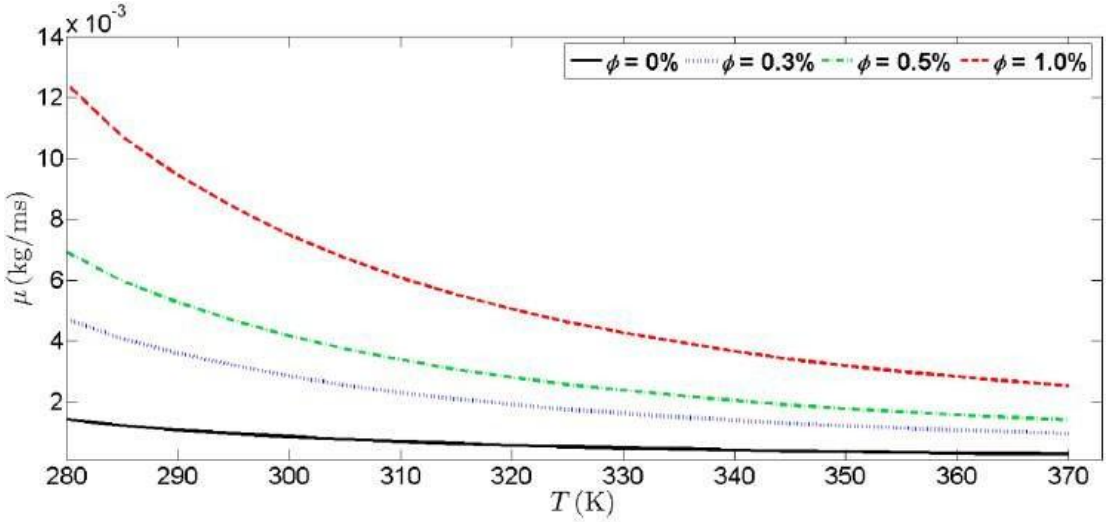


Fig.7. Viscosity of GnP-water nanofluid with respect to temperature for various ϕ

3.2 Grid Independence Study

Grid independence studies were performed to identify the optimal mesh size for the current investigation. ANSYS Fluent Meshing was employed to generate the mesh, producing six distinct mesh sizes for the determination of $\overline{Nu}$ for both basefluid and GnP-water nanofluid in a microtube radiator, with Re = 100 and T_i = 333 K. The specific mesh sizes are shown in Table 3.

Table 3
Mesh sizes for grid independence study

Grid	Nodes	Elements
Mesh 1	17 063	14 250
Mesh 2	49 196	43 000
Mesh 3	106 002	95 200
Mesh 4	193 930	177 300
Mesh 5	332 804	308 550
Mesh 6	507 780	475 150

Figure 6 shows the $\overline{Nu}$ of the six meshes for ϕ = 0% and ϕ = 0.5%. It is notable that the $\overline{Nu}$ for all mesh configurations are similar for both fluids. As shown in Figure 8, the lowest percentage difference in the results for the basefluid occurs between mesh 5 and mesh 6, at 0.73%. In contrast, the lowest percentage difference for the GnP-water nanofluid is observed between mesh 3 and mesh 4, at 0.98%. Since grid independence for the basefluid is achieved with mesh 5, simulations for the microtube radiator were conducted using this mesh. The meshing layout for mesh 5 is depicted in Figure 1, with a symmetry boundary condition applied to reduce mesh size and computational time.

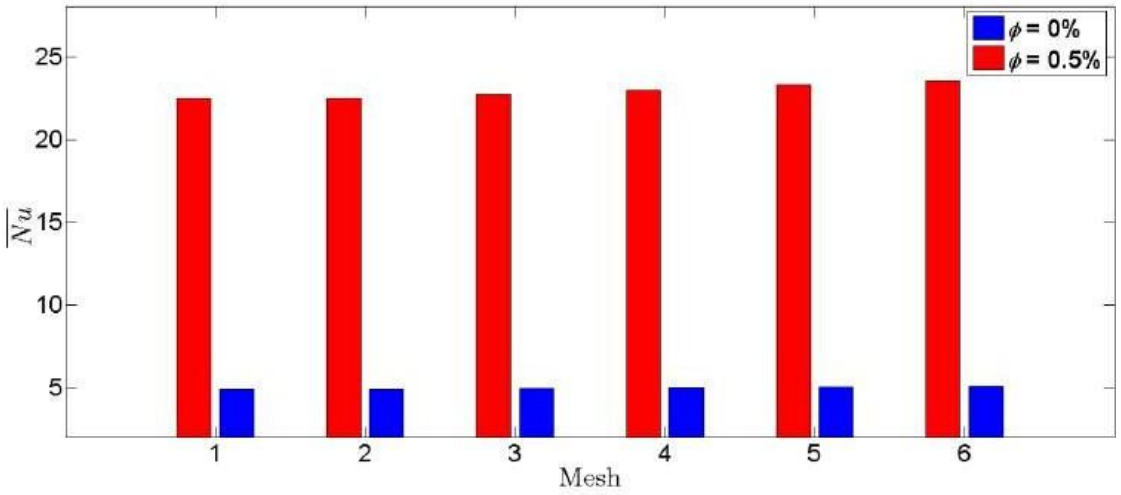
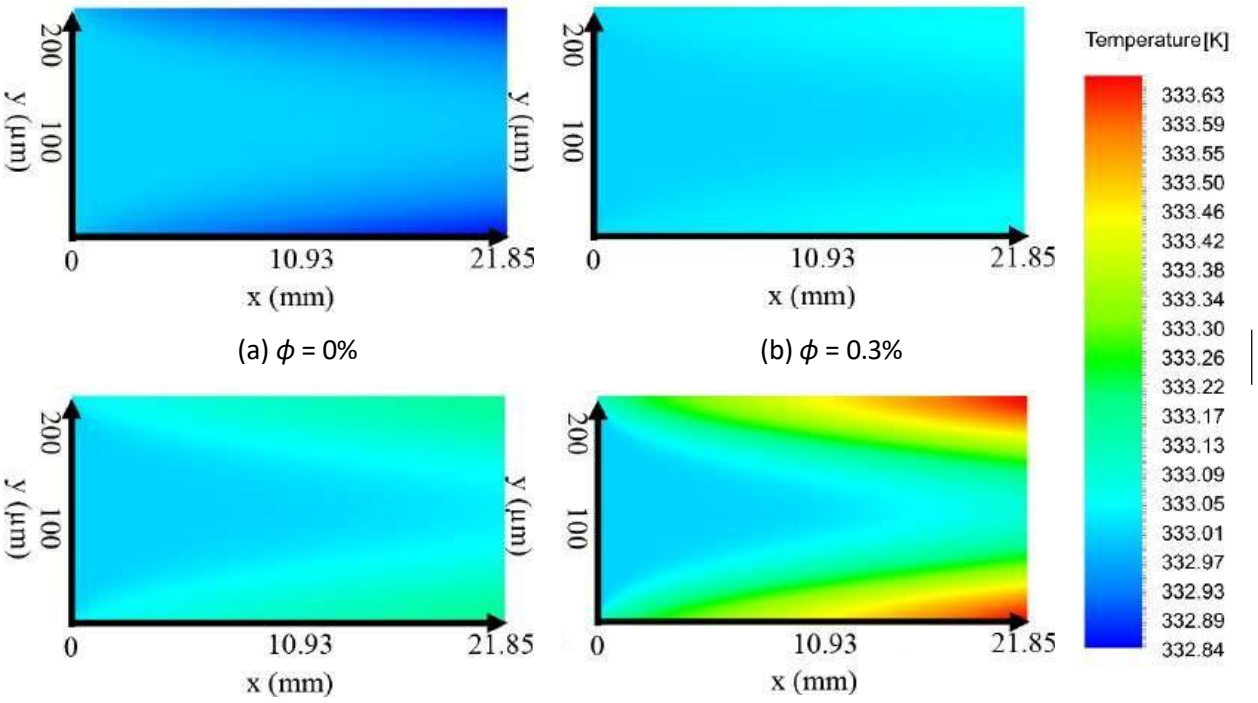


Fig.8. Average Nusselt number of various mesh size for ϕ = 0% and ϕ = 0.5%

3.3 Effect of Reynolds Number

The study on the influence of Reynolds number in a microtube radiator using GnP-water nanofluid was conducted with various Re values with T_i = 333 K. Figure 9 displays the temperature contours for both basefluid and GnP-water nanofluid within the microtube radiator. In the basefluid case, as shown in Figure 9(a), the temperature profile decreases along the channel. Conversely, for the GnP-water nanofluid, illustrated in Figure 9(b) to Figure 9(d), the temperature profile increases along the channel, which can be attributed to the effect of viscous dissipation. This phenomenon

occurs when frictional heat generated by fluid-wall interactions raises the fluid's temperature [53], causing heating instead of cooling in the microtube radiator when GnP-water nanofluid is used as the coolant. Under viscous dissipation, the fluid temperature exceeds that of the wall, resulting in a negative wall heat flux and a subsequent decline in heat transfer performance. Comparing Figure 9(b) and Figure 9(c), the GnP-water nanofluid with lower concentrations shows a smaller streamwise temperature gradient along the channel compared to higher-concentration GnP-water nanofluid. The reduced T_w - T_b leads to a smaller heat transfer coefficient, as indicated in Eq. (21). T_w - T_b increases with the increase of ϕ, which possibly leads to higher heat transfer coefficient, as demonstrated in Figure 9 and Eq. (21). In microtube radiator, the viscous dissipation effect intensifies with the increase of ϕ.



(a) ϕ = 0% (b) ϕ = 0.3%

(c) ϕ = 0.5% (d) ϕ = 1.0%

Fig.9. Temperature contour of GnP nanofluid with (a) ϕ = 0%, (b) ϕ = 0.3%, (c) ϕ = 0.5% and (d) ϕ = 1.0%

Figure 10 illustrates the average Nusselt number $\overline{Nu}$ over the entire tube length for various Re and ϕ in a microtube radiator. When Re≤100, $\overline{Nu}$ increases with both higher GnP suspension concentrations and Re, consistent with the behavior observed in millimeter-sized radiators as reported by Toh et al. [22]. Hung [54] also noted that nanofluid heat transfer performance improves with increasing nanoparticle concentration. As shown in Table 4, the enhancement of $\overline{Nu}$ of the present study for ϕ = 1.0% GnP-water nanofluid with Re = 1 and Re = 100 are 572.92% and 1063.27% respectively. Shi et al. [55] similarly found that heat transfer performance in microchannels improves with increasing Re and nanoparticle concentration.

Table 4
The enhancement of $\overline{Nu}$

Reynolds Number	Nusselt Number		Percentage of Enhancement
	Base Fluid	GnP-water nanofluid with ϕ = 1.0%	
1	5.36	30.69	573%
100	5.51	58.59	1063%

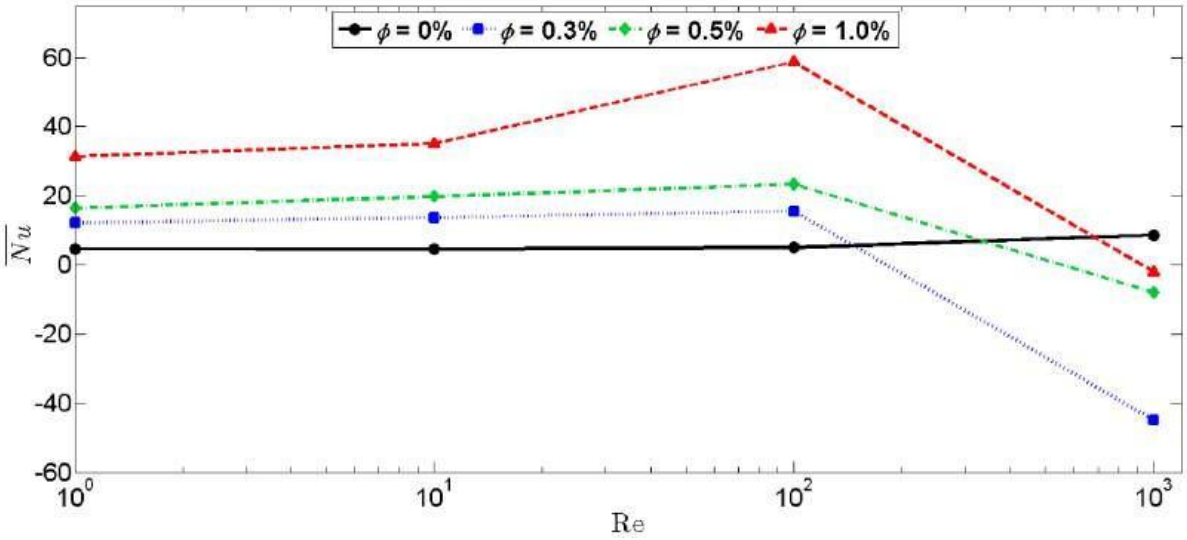


Fig.10. Variation of $\overline{Nu}$ with Re for different ϕ

Based on Figure 10, GnP-water nanofluid with Re>100 exhibits reduced thermal performance due to viscous dissipation effects, which become increasingly significant at high Re, leading to thermal performance deterioration [53]. Viscous dissipation refers to the conversion of mechanical energy into thermal energy as a result of internal fluid friction during flow. In microtube geometries, the effect becomes more pronounced due to the relatively large velocity gradients near the tube walls. As the Reynolds number increases, the shear stresses within the fluid intensify, generating additional heat inside the fluid domain. This internally generated heat reduces the effective temperature difference between the heated wall and the flowing fluid, which weakens the convective heat transfer and leads to a reduction in overall thermal performance. Among the GnP-water nanofluid concentrations studied, the ϕ = 0.3% suspension shows the lowest $\overline{Nu}$ at higher Re = 1000 compared to ϕ = 0.5% and ϕ = 1.0% suspensions. This result aligns with Figure 9, where the ϕ = 0.3% nanofluid exhibits a smaller streamwise temperature difference along the channel under viscous dissipation than the ϕ = 0.5% suspension, resulting in a reduced $\overline{Nu}$. Under the effect of viscous dissipation, with increased ϕ, the effect of viscous dissipation intensifies, raising the streamwise temperature difference along the channel and thereby increasing $\overline{Nu}$. In microtube radiators, the ϕ = 1.0% GnP-water nanofluid at Re = 1000 demonstrates the strongest viscous dissipation effect. The nanofluid shows improved thermal performance in microchannels at low Re but experiences performance degradation at high Re due to this dissipation effect [56]. Conversely, the basefluid is unaffected by viscous dissipation at high Re, owing to its lower viscosity and thermophysical properties. Its heat transfer performance improves as Re increases, with an 84.66% enhancement in $\overline{Nu}$ as Re rises from 1 to 1000. Therefore, the basefluid demonstrates superior thermal performance in microtube radiators at high Reynolds numbers compared to GnP-water nanofluid, due to the minimal impact of viscous dissipation in the basefluid flow.

3.4 Effect of Inlet Temperature

Figure 11 presents the variations $\overline{Nu}$ with T_i in a microtube radiator using GnP-water nanofluid with Re = 10 and Re = 1000. The $\overline{Nu}$ for the basefluid at Re = 1000 increases as the inlet temperature decreases. Under the influence of viscous dissipation, GnP-water nanofluid at Re = 1000 exhibits a higher $\overline{Nu}$ as the inlet temperature decreases, attributed to the increased viscosity at lower

temperatures, as shown in Figure 7. According to Eq. (20), both Re and inlet velocity are significantly affected by viscosity; under constant Re, inlet velocity increases as viscosity rises [22]. Higher ϕ amplify the viscous dissipation effect. Accordingly, the $\overline{Nu}$ for GnP-water nanofluid with ϕ = 1.0% is 87.24% greater than that for ϕ = 0.3% at 318 K. The thermal performance of the nanofluid in microtube deteriorates due to viscous dissipation effects [54]. For ϕ = 0.5% GnP-water nanofluid at 318 K and 333 K, $\overline{Nu}$ are -1.80 and -8.13, respectively, reflecting a performance decrease of up to 351.33%. This suggests that, at high Re, the effect of increased viscosity outweighs thermal conductivity benefits. For example, despite its higher thermal conductivity, the basefluid at T_i = 333 K exhibits a 50.46% lower $\overline{Nu}$ than T_i = 318 K, underscoring the dominant influence of viscosity over thermal conductivity in microtube radiators at high Re. Thus, the basefluid proves more effective at high Re and low inlet temperatures in microtube radiators, as the viscous dissipation effect in GnP-water nanofluid adversely impacts its thermal performance in these conditions.

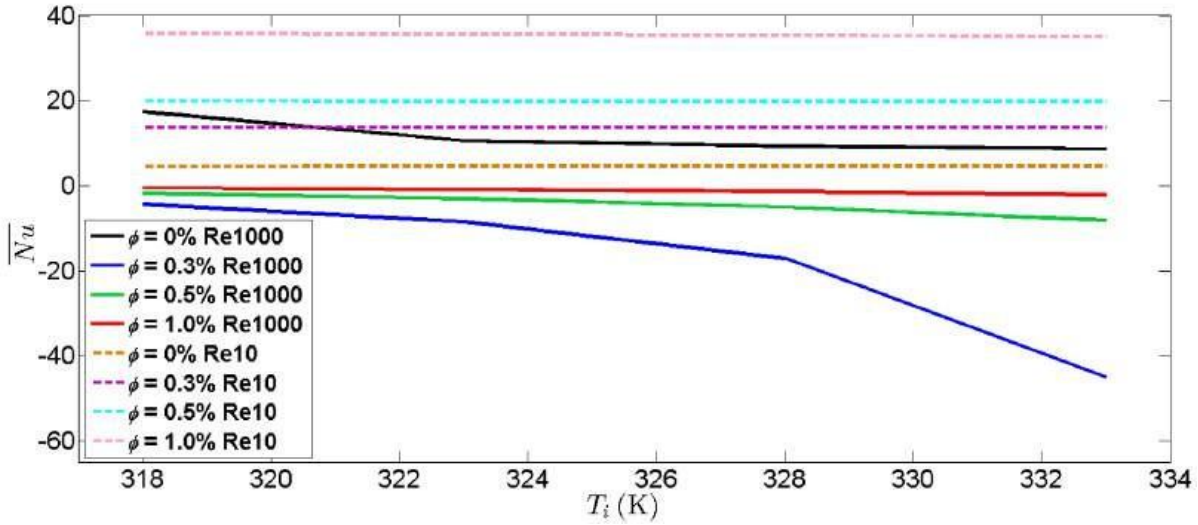


Fig.11. Variation of $\overline{Nu}$ with T_i for different ϕ and Re

As shown in Figure 11, at Re = 10, the effects of inlet temperature on the thermal performance variation of GnP-water nanofluid in a microtube radiator is minimal. The result shows a slight reduction of $\overline{Nu}$ with the increase of T_i, concurring with that reported by Toh *et al.* [22]. When inlet temperature rises from 318 K to 333 K, Nusselt number decreases by 1.73% for GnP-water nanofluid with ϕ = 1.0%. The effects of T_i in microtube radiator is more significant at high-Re flow as compared to low-Re flow. GnP-water nanofluid demonstrates an increase in the Nusselt number with greater GnP nanoparticle suspension at Re = 10. The enhancement of $\overline{Nu}$ is 682.86% for GnP-water nanofluid with ϕ = 1.0% and T_i = 318 K as compared to the basefluid. This improvement can be attributed to the increased thermal conductivity resulting from the GnP suspension [27]. When the effect of viscous dissipation is insignificant at low-Re flow, GnP-water nanofluid shows a better thermal performance of the microtube radiator as compared to basefluid.

3.5 Effect of Nanoparticles Thickness

The effects of GnP nanoparticles thickness, t_p on the performance of microtube radiators were evaluated at D_p = 2 µm and T_{in} = 318 K. The ideal interface assumption is applied to the thermal conductivity, and all thermophysical properties of nanofluids with the various t_p are computed using Eq. (4) and Eq. (19). Figure 12 presents $\overline{Nu}$ with varying t_p at Re = 10 and Re = 1000. It is observed

that the basefluid is unaffected by changes in t_p. However, GnP-water nanofluid demonstrates a decline in heat transfer performance at Re = 1000, as shown in Figure 12(a). Under conditions of viscous dissipation, the GnP-water nanofluid exhibits higher Nusselt numbers with decreasing t_p and increasing ϕ. When t_p = 1nm, the $\overline{Nu}$ for ϕ = 0.3% and ϕ = 1.0% GnP-water nanofluid are -0.69 and -0.097, respectively. The increase of the $\overline{Nu}$ for ϕ = 1.0% Gnp-water nanofluid with t_p decreased from 4 nm to 1 nm is 96.89%. This enhancement is attributed to the significant increase in viscosity of the GnP-water nanofluid with decreasing t_p, which augments the viscous dissipation effect. The increase of the viscosity for ϕ = 1.0% GnP-water nanofluid with t_p reduced from 4 nm to 1 nm is 413.93% at the temperature of 318 K. Despite this, the improvement in thermal conductivity is minimal due to the dominant viscous dissipation effect at high-Re flow. At high-Re flow, the basefluid exhibits superior heat transfer performance compared to the GnP-water nanofluid, with the suspension of GnP nanoparticles diminishing the thermal performance of the microtube radiator.

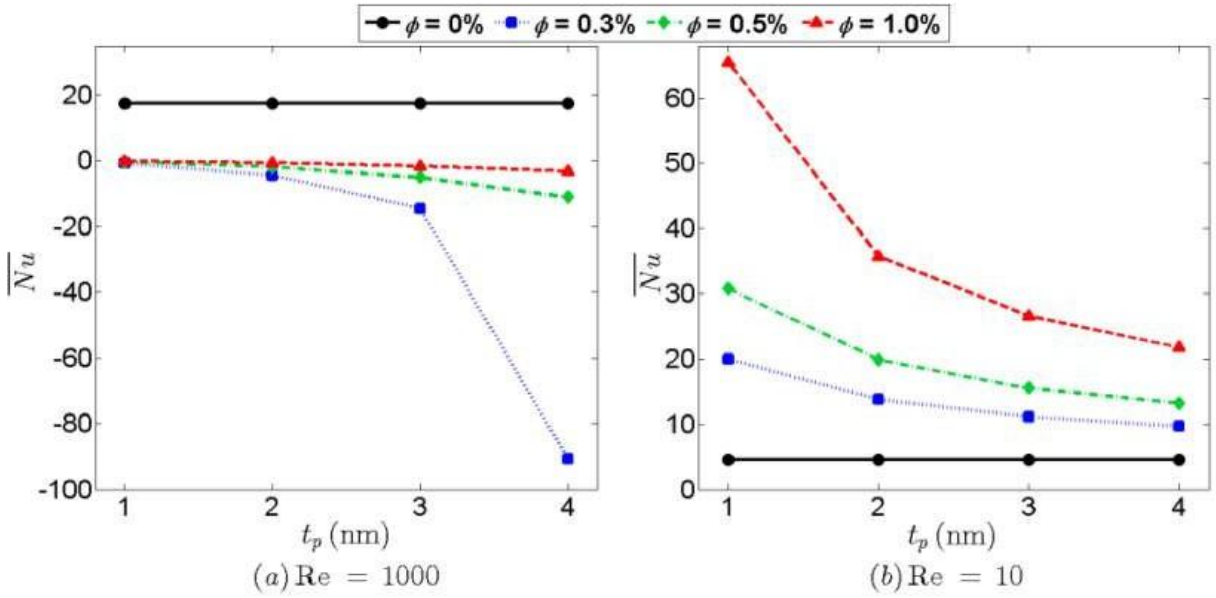


Fig.12. Variation of $\overline{Nu}$ with t_p for different ϕ at (a) Re = 1000 and (b) Re = 10

As shown in Figure 12(b), the heat transfer performance improves with decreasing t_p and increasing ϕ at Re = 10. The ϕ = 1.0% GnP-water nanofluid achieved a peak Nusselt number of 65.52 at t_p = 1 nm. The enhancement in Nusselt number for GnP-water nanofluids with 0.3 vol.% and 1.0 vol.% concentration, as the particle thickness decreased from 4 nm to 1 nm, was 106.86% and 201.85%, respectively, which aligns with findings for millimeter-sized radiators [22]. At low Reynolds numbers, GnP-water nanofluid demonstrated superior heat transfer performance over the basefluid. Studies by Sadaghiani et al. [57] and Anoop et al. [58] also indicate that heat transfer performance increases with smaller nanoparticle size, attributed to enhanced thermal conductivity and viscosity as particle thickness decreases. Increased inlet velocity can further enhance this heat transfer performance. Decreasing particle thickness increases the contact area between particles and fluid, thereby enhancing heat transfer [59]. Moreover, intensified Brownian motion effects further contribute to this improvement [60].

3.6 Effect of Tube Diameter

The influence of tube diameter, D on GnP-water nanofluid in microtube radiators was investigated at L = 21.85 mm and T_{in} = 318 K. Figure 13 presents the average Nusselt number over the tube length, demonstrating how different tube diameters affect heat transfer performance in the microtube radiator at Re = 1000. The basefluid shows a decrease in Nusselt number as tube diameter increases. As tube diameter increases, the cross-sectional area expands, reducing the inlet velocity (for a constant Reynolds number) and subsequently diminishing heat transfer performance [61]. For the basefluid, increasing the tube diameter from 200 µm to 350 µm results in a 33.60% decrease in the Nusselt number. For GnP-water nanofluid, heat transfer performance also declines due to the viscous dissipation effect. The Nusselt number decreases with both increasing tube diameter and decreasing GnP concentration. Specifically, the reduction in Nusselt number for GnP-water nanofluids with 0.3 vol.% and 1.0 vol.% concentration when the tube diameter increases from 250 µm to 300 µm is 170.84% and 76.68%, respectively. Increasing the GnP concentration from 0.5 vol.% to 1.0 vol.% enhances the Nusselt number by 75.87% at D = 350 µm. When D = 300 µm, 0.3 vol.% GnP-water nanofluid exhibits the lowest Nusselt number due to the lowest of T_w - T_b, as shown by Eq. (21).

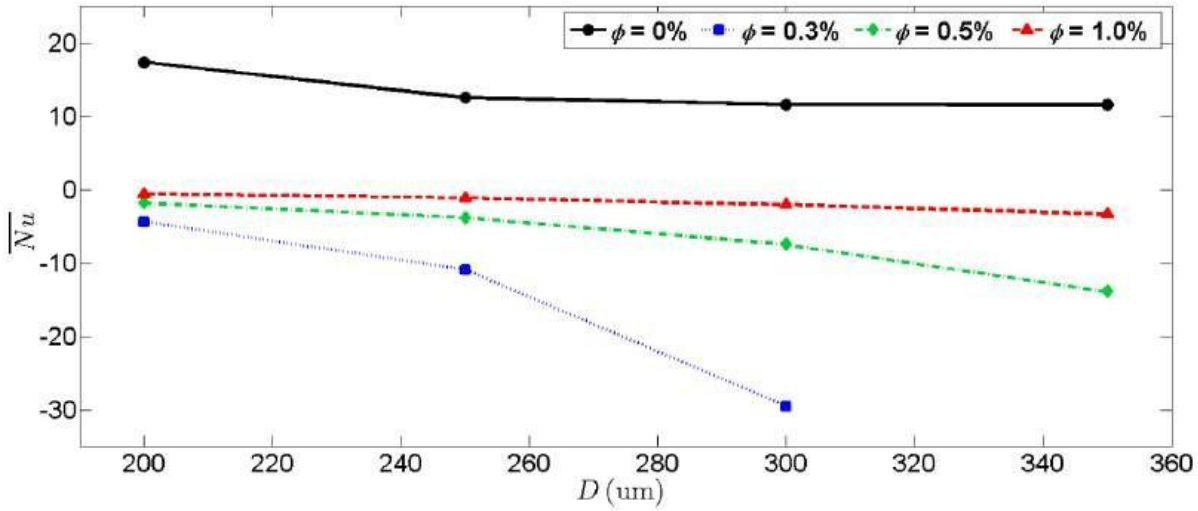
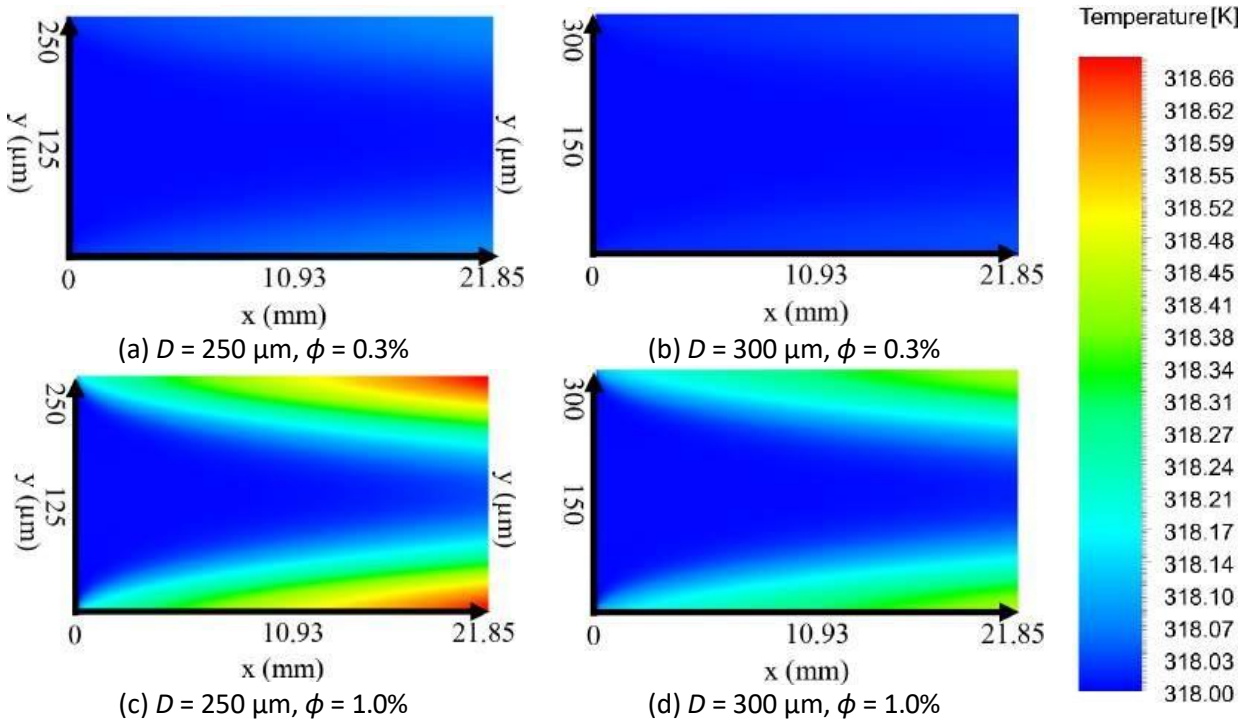


Fig.13. Variation of $\overline{Nu}$ with D for different ϕ at Re = 1000

Figure 14 displays temperature contours for 0.3 vol.% and 1.0 vol.% GnP-water nanofluids in microtube radiators with different tube diameters at Re = 1000. The temperature profile within the channel increases due to viscous dissipation, which involves the irreversible conversion of kinetic energy into thermal energy through fluid friction. In microtubes, this effect is intensified by steep near-wall velocity gradients. At higher Reynolds numbers, increased shear stresses act as a volumetric heat source, elevating the bulk fluid temperature. This reduces the thermal gradient between the wall and the fluid, thereby suppressing the convective heat transfer driving force and deteriorating overall performance. Figure 14(b) and Figure 14(d) illustrate a reduced temperature gradient along the channel as tube diameter increases, in contrast to Figure 14(a) and Figure 14(c). Figure 14(a) and Figure (b) illustrate the bulk temperature T_b approaching the wall temperature T_w. According to Hung [54], this occurs when the fluid's heat transfer is offset by the heat generated from viscous dissipation, bringing T_b and T_w closer together. This reduces the heat transfer between the wall and the fluid, which can result in the Nusselt number approaching infinity [54]. Therefore, as

illustrated in Figure 13, the GnP-water nanofluid with a 0.3 vol.% concentration exhibits the lowest Nusselt number at D = 300 µm when the fluid's heat transfer is balanced by the heat generated from viscous dissipation. As the GnP concentration increases, the streamwise temperature gradient also increases, as observed in Figure 14(a) and Figure 14(c). This leads to a higher Nusselt number for the 1.0 vol.% GnP-water nanofluid compared to the 0.3 vol.% suspension, as depicted in Figure 13. As particle thickness decreases and GnP concentration increases, the viscous dissipation effect intensifies, further diminishing the thermal performance of the microtube radiators. Overall, basefluid demonstrates better heat transfer in smaller tube diameters under high-Re flow compared to GnP-water nanofluid.



(a) D = 250 µm, ϕ = 0.3% (b) D = 300 µm, ϕ = 0.3%

(c) D = 250 µm, ϕ = 1.0% (d) D = 300 µm, ϕ = 1.0%

Fig.14. Temperature contour of GnP nanofluid with Re = 1000

Figure 15 illustrates the average heat transfer coefficient over the entire tube length, $\bar{h}$ for various tube diameters, D in a microtube radiator at Re = 10. The GnP-water nanofluid demonstrates better thermal performance compared to the basefluid. The heat transfer coefficient decreases with increasing tube diameter and decreasing GnP concentration. The heat transfer coefficient for both the basefluid and the 1.0 vol.% GnP-water nanofluid increases by 42.10% and 42.90%, respectively, as the tube diameter decreases from 350 µm to 200 µm. This behavior is similar to that observed in millimeter-sized radiators [22]. At low-Re flow, GnP-water nanofluid enhances the thermal performance of the microtube radiator, as the viscous dissipation effect is negligible and does not degrade heat transfer performance [54]. At D = 350 µm, the heat transfer coefficient for 0.3 vol.% and 1.0 vol.% GnP-water nanofluids increases by 214.24% and 705.61%, respectively, relative to the basefluid. The effect of GnP concentration outweighs that of tube diameter, primarily due to the superior enhancement in thermal conductivity.

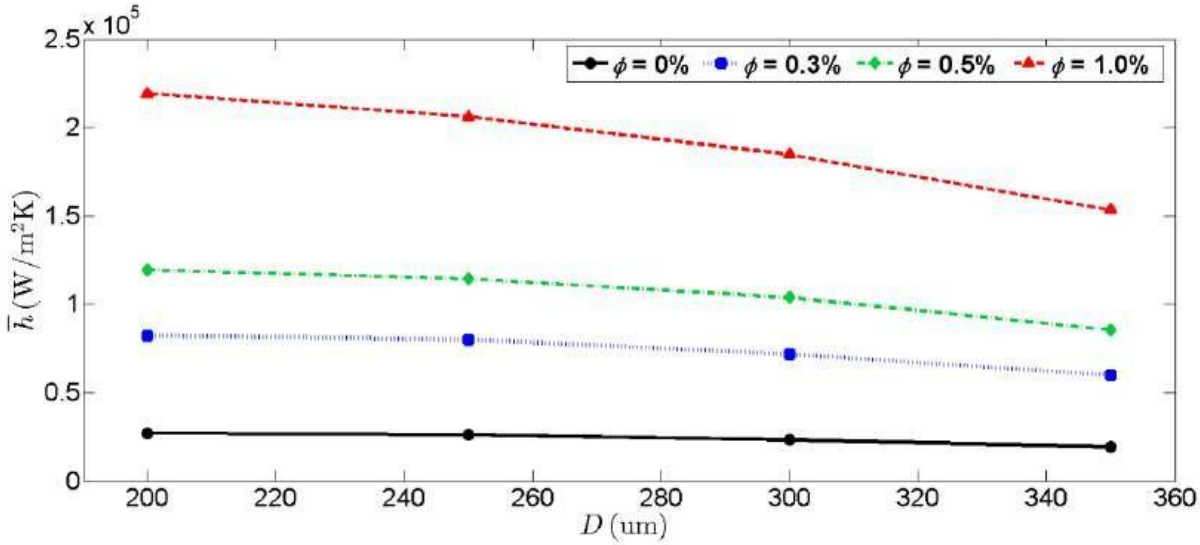


Fig.15. Variation of $\bar{h}$ with D for different ϕ at Re = 10

Despite the promising results obtained in this study, several limitations should be acknowledged. First, the present work is based solely on numerical simulations using ANSYS Fluent, and experimental validation has not yet been conducted. Therefore, future studies should include experimental investigations to verify the predicted heat transfer enhancement. Second, the long-term stability of graphene nanoplatelet nanofluids may present practical challenges in real applications, including potential nanoparticle agglomeration and sedimentation during extended operation. These factors may influence the thermal performance and reliability of nanofluid-based cooling systems. Future research should therefore investigate nanoparticle dispersion stability and evaluate the performance of GnP nanofluids under realistic operating conditions in automotive radiator systems.

4. Conclusions

This study presents a comprehensive analysis of the convection performance of microtube automotive radiators using GnP-water nanofluids. The temperature-dependent thermophysical properties of GnP-water nanofluids, including density, specific heat capacity, and viscosity, were evaluated to assess the impact of nanoparticles suspension on the heat transfer performance of the radiator. Increasing the GnP concentration leads to an increase in the density of the nanofluid, while the specific heat capacity decreases. However, the thermal conductivity of the GnP-water nanofluid increased significantly, up to 667.16% compared to the basefluid. The viscosity of the nanofluid decreased with increasing temperature but increased with increasing particle concentration, reaching up to 774.34% higher than that of the base fluid. In the microtube radiator, the heat transfer performance improved with increasing GnP concentration and Reynolds number when Re≤100. However, at Re>100, the performance deteriorated due to the viscous dissipation effect, which becomes more pronounced as the GnP loading increases. In these conditions, the basefluid showed better thermal performance. At Re = 1000, decreasing inlet temperature increases the Nusselt number for GnP-water nanofluids. At Re = 10, both GnP concentration and decreasing inlet temperature enhance the Nusselt number, though the temperature's effect is smaller than GnP concentration. The study also examined the impact of nanoparticle thickness and tube diameter on the radiator's performance. It was found that decreasing the nanoparticle thickness and increasing the GnP concentration enhanced the heat transfer. On the other hand, at Re = 1000, Nusselt number decreases with increasing tube diameter and decreasing GnP loading, due to the viscous dissipation

effect. The basefluid performs better as tube diameter decreases. However, at Re = 10, both the GnP-water nanofluid and the basefluid show improved heat transfer with reduced tube diameter and increased GnP concentration. Overall, the GnP-water nanofluid demonstrated superior thermal performance compared to the basefluid at low-Re flow in microtube radiators. However, at high-Re flow, the viscous dissipation effect diminished the advantages of the nanofluid. The basefluid proved more effective at high-Re flow. These findings highlight the potential of GnP-water nanofluids in improving the thermal performance of microtube automotive radiators, particularly in applications with low flow rates, contributing to more efficient radiators and better fuel efficiency. Despite the promising findings, further research is recommended to extend the present study. Experimental investigations are required to validate the numerical results and to confirm the predicted heat transfer enhancement in practical radiator systems. In addition, future studies should focus on optimizing the nanoparticle concentration to achieve an optimal balance between thermal performance improvement and viscosity-related penalties. The stability and long-term operational behavior of GnP–water nanofluids should also be examined, as nanoparticle agglomeration and sedimentation may affect their performance and reliability in real automotive cooling systems. Addressing these aspects will help facilitate the practical implementation of GnP-based nanofluids in advanced microtube radiator applications.

Acknowledgement
This research was funded by University Research Grant from University of Technology Sarawak (UTS/RESEARCH/4/2023/05).

References

[1] An, F., Earley, R., and Green-Weiskel, L. (2011). *Global overview on fuel efficiency and motor vehicle emission standards: Policy options and perspectives for international cooperation*. United Nations Department of Economic and Social Affairs.
[2] Poder, T.G. and He, J. "Willingness to pay for a cleaner car: The case of car pollution in Quebec and France." *Energy* 130 (2019): 48-54. doi: https://doi.org/10.1016/j.energy.2017.04.107
[3] World Energy Scenarios: Global Transport Scenarios 2050, World Energy Council, 2011.
[4] U.S. Energy Information Administration. (2017). *Global Transportation Energy Consumption: Examination of Scenarios to 2040 using ITEDD*.
[5] Georgios Fontaras, Nikiforos-Georgios Zacharof, and Biagio Ciuffo. "Fuel consumption and CO2 emissions from passenger cars in Europe – Laboratory versus real-world emissions." *Progress in Energy and Combustion Science* 60 (2017): 97-131. https://doi.org/10.1016/j.pecs.2016.12.004
[6] Vajjha, R.S., Das, D.K., and Namburu, P.K. "Numerical study of fluid dynamic and heat transfer performance of Al2O3 and CuO nanofluids in the flat tubes of a radiator." *International Journal of Heat and Fluid Flow* 31, no. 4 (2010): 613-621. https://doi.org/10.1016/j.ijheatfluidflow.2010.02.016
[7] Huong, N.H., Ting, T.W., Toh, L.K.L., and Ngu, H.J. "Experimental study on convective heat transfer enhancement of automotive radiator with graphene-nanoplatelet suspension." *Journal of Advanced Research in Fluid Mechanics and Thermal Sciences* 101, no. 2 (2023): 60-72. https://doi.org/10.37934/arfmts.101.2.6072
[8] Harun, M.A., Che Sidik, N.A., Yutaka, A., and Tan Lit, K. "Recent review on preparation method, mixing ratio, and heat transfer application using hybrid nanofluid." *Journal of Advanced Research in Fluid Mechanics and Thermal Sciences* 95, no. 1 (2022): 44-53. https://doi.org/10.37934/arfmts.95.1.4453
[9] Irwansyah, R., Rahmadiawan, D., Gasni, D., and Raynaldo, K. "Numerical Investigation of Ti3C2 MXene Nanofluid Convective Heat Transfer Performance in Circular Tube." *CFD Letters* 17, no. 7 (2025): 130-141. https://doi.org/10.37934/cfdl.17.7.130141
[10] Selvam, C., Mohan Lal, D., and Harish, S. "Enhanced heat transfer performance of an automobile radiator with graphene based suspensions." *Applied Thermal Engineering* 123 (2017): 50-60. https://doi.org/10.1016/j.applthermaleng.2017.05.076
[11] Che Halim, N.F., and Che Sidik, N.A. "Nanorefrigerants: A review on thermophysical properties and their heat transfer performance." *Journal of Advanced Research in Applied Sciences and Engineering Technology* 20, no. 1 (2020): 42-50. https://doi.org/10.37934/araset.20.1.4250

[12] Abdul Raqib, M., Alaiwi, Y., and Jundi, A.. "Numerical Investigation of Thermal Performance Enhancement in a Newly Designed Shell and Tube Heat Exchanger using TiO2 Nanofluids." *CFD Letters* 17, no. 2 (2025): 60-82. https://doi.org/10.37934/cfdl.17.2.6082
[13] Tuaima, A.N., Shkaraha, A.J., and Salman, M.D. "An Experimental and Numerical Study of the Effect of Microchannels Geometry on Heat Transfer of Nanofluids." *CFD Letters* 16, no. 7 (2024): 89-104. https://doi.org/10.37934/cfdl.16.7.89104
[14] M'Hamed, B., Che Sidik, N.A., Akhbar, M.F.A., Mamat, R., and Najafi, G. "Experimental study on thermal performance of MWCNT nanocoolant in Perodua Kelisa 1000cc radiator system." *International Communications in Heat and Mass Transfer* 76 (2016): 156-161. https://doi.org/10.1016/j.icheatmasstransfer.2016.05.024
[15] Che Sidik, N.A., Witri Mohd Yazid, M.N.A., and Mamat, R. "Recent advancement of nanofluids in engine cooling system." *Renewable and Sustainable Energy Reviews* 75 (2017): 137-144. https://doi.org/10.1016/j.rser.2016.10.057
[16] Patel, J., Soni, A., Barai, D.P., and Bhanvase, B.A. "A minireview on nanofluids for automotive applications: Current status and future perspectives." *Applied Thermal Engineering* 219 (2023): 119428. https://doi.org/10.1016/j.applthermaleng.2022.119428
[17] Sciences, X., *xGnP Graphene Nanoplatelets-Grade M Techincal Data Sheet*. 2015.
[18] Awad, A.T., Yaseen, A.H., and Hussein, A.M. "Evaluation of Heat Transfer and Fluid Dynamics across a Backward Facing Step for Mobile Cooling Applications Utilizing CNT Nanofluid in Laminar Conditions." *CFD Letters* 16, no. 10 (2024): 140-153. https://doi.org/10.37934/cfdl.16.10.140153
[19] Naveen, N.S., and Kishore, P.S. "Experimental investigation on heat transfer parameters of an automotive car radiator using graphene/water-ethylene glycol coolant." *Journal of Dispersion Science and Technology* 43, no. 3 (2022): 1-13. https://doi.org/10.1080/01932691.2020.1840999
[20] Yaw, C.T., Koh, S.P., Sandhya, M., Kadirgama, K., Tiong, S.K., Ramasamy, D., Sudhakar, K., Samykano, M., Benedict, F., and Tan, C.H. "Heat transfer enhancement by hybrid nano additives-graphene nanoplatelets/cellulose nanocrystal for the automobile cooling system (Radiator)." *Nanomaterials* 13, no. 5 (2023): 808. https://doi.org/10.3390/nano13050808
[21] Ponangi, B.R., Krishna, V., and Seetharamu, K.N. "Performance of compact heat exchanger in the presence of novel hybrid graphene nanofluids." *International Journal of Thermal Sciences* 165 (2021): 106925. https://doi.org/10.1016/j.ijthermalsci.2021.106925
[22] Toh, L.K.L., and Ting, T.W. "Numerical Simulation of Graphene-Nanoplatelet Nanofluid Convection in Millimeter-Sized Automotive Radiator." *CFD Letters* 16, no. 6 (2024): 32-52. https://doi.org/10.37934/cfdl.16.6.3252
[23] Ting, T.W., Hung, Y.M., and Guo, N. "Viscous dissipative forced convection in thermal non-equilibrium nanofluid-saturated porous media embedded in microchannels." *International Communications in Heat and Mass Transfer* 57 (2014): 309-318. https://doi.org/10.1016/j.icheatmasstransfer.2014.08.018
[24] Fani, B., Kalteh, M., and Abbassi, A. "Investigating the effect of Brownian motion and viscous dissipation on the nanofluid heat transfer in a trapezoidal microchannel heat sink." *Advanced Powder Technology* 26, no. 1 (2015): 83-90. https://doi.org/10.1016/j.apt.2014.08.009
[25] Nimmagadda, R., and Venkatasubbaiah, K. "Conjugate heat transfer analysis of micro-channel using novel hybrid nanofluids (Al2O3+Ag/Water)." *European Journal of Mechanics - B/Fluids* 52 (2015): 19-27. https://doi.org/10.1016/j.euromechflu.2015.01.007
[26] Akhai, S., and Wadhwa, A. "Enhancing Radiator Cooling with CuO Nanofluid Microchannels." *International Journal of Automotive Science And Technology* 8, no. 2 (2024): 201-211. https://doi.org/10.30939/ijastech. 1399702
[27] Selvam, C., Solaimalai Raja, R., Mohan Lal, D., and Harish, S. "Overall heat transfer coefficient improvement of an automobile radiator with graphene based suspensions." *International Journal of Heat and Mass Transfer* 115 (2017): 580-588. https://doi.org/10.1016/j.ijheatmasstransfer.2017.08.071
[28] Ajuka, L.O., Ikumapayi, O.M., and Akinlabi, E.T. "Entropy Generation of Graphene Nanoplatelets in Micro and Mini Channels: Nanofluid Flow in Automotive Cooling Applications." *International Journal of Heat and Technology* 40, no. 4 (2022): 917-926. https://doi.org/10.18280/ijht.400408
[29] Naraki, M., Peyghambarzadeh, S.M., Hashemabadi, S.H., and Vermahmoudi, Y. "Parametric study of overall heat transfer coefficient of CuO/water nanofluids in a car radiator." *International Journal of Thermal Sciences* 66 (2013): 82-90. https://doi.org/10.1016/j.ijthermalsci.2012.11.013
[30] Elsebay, M., Elbadawy, I., Shedid, M.H., and Fatouh, M. "Numerical resizing study of Al2O3 and CuO nanofluids in the flat tubes of a radiator." *Applied Mathematical Modelling* 40, no. 13 (2016): 6437-6450. https://doi.org/10.1016/j.apm.2016.01.039
[31] Pak, B.C., and Cho, Y.I. "Hydrodynamic and heat transfer study of dispersed fluids with submicron metallic oxide particles." *Experimental Heat Transfer* 11, no. 2 (1998): 151-170. https://doi.org/10.1080/08916159808946559

[32] Xuan, Y., and Roetzel, W. "Conceptions for heat transfer correlation of nanofluids." *International Journal of Heat and Mass Transfer* 43, no. 19 (2000): 3701-3707. https://doi.org/10.1016/S0017-9310(99)00369-5
[33] Zhao, N., Yang, J., Li, H., Zhang, Z., and Li, S. "Numerical investigations of laminar heat transfer and flow performance of Al2O3–water nanofluids in a flat tube." *International Journal of Heat and Mass Transfer* 92 (2016): 268-282. https://doi.org/10.1016/j.ijheatmasstransfer.2015.08.098
[34] Peyghambarzadeh, S.M., Hashemabadi, S.H., Hoseini, S.M., and Seifi Jamnani, M. "Experimental study of heat transfer enhancement using water/ethylene glycol based nanofluids as a new coolant for car radiators." *International Communications in Heat and Mass Transfer* 38, no. 9 (2011): 1283-1290. doi: https://doi.org/10.1016/j.icheatmasstransfer.2011.07.001
[35] Selvam, C., Balaji, T., Mohan Lal, D., and Harish, S. "Convective heat transfer coefficient and pressure drop of water-ethylene glycol mixture with graphene nanoplatelets." *Experimental Thermal and Fluid Science* 80 (2017): 67-76. https://doi.org/10.1016/j.expthermflusci.2016.08.013
[36] Sadeghinezhad, E., Togun, H., Mehrali, M., Sadeghi Nejad, P., Tahan Latibari, S., Abdulrazzaq, T., Kazi, S.N., and Metselaar, H.S.C. "An experimental and numerical investigation of heat transfer enhancement for graphene nanoplatelets nanofluids in turbulent flow conditions." *International Journal of Heat and Mass Transfer* 81 (2015): 41-51. https://doi.org/10.1016/j.ijheatmasstransfer.2014.10.006
[37] Ahammed, N., Asirvatham, L.G., and Wongwises, S. "Effect of volume concentration and temperature on viscosity and surface tension of graphene–water nanofluid for heat transfer applications." *Journal of Thermal Analysis and Calorimetry* 123, no. 2 (2016): 1399-1409. https://doi.org/10.1007/s10973-015-5034-x
[38] Nan, C.-W., Birringer, R., Clarke, D.R., and Gleiter, H. "Effective thermal conductivity of particulate composites with interfacial thermal resistance." *Journal of Applied Physics* 81, no. 10 (1997): 6692-6699. https://doi.org/10.1063/1.365209
[39] Park, K.W., and Pak, H.Y. "Flow and heat transfer characteristics in flat tubes of a radiator." *Numerical Heat Transfer, Part A: Applications* 41, no. 1 (2002): 19-40. https://doi.org/10.1080/104077802317221429
[40] Ting, T.W., Hung, Y.M., and Guo, N. "Viscous dissipative nanofluid convection in asymmetrically heated porous microchannels with solid-phase heat generation." *International Communications in Heat and Mass Transfer* 68 (2015): 236-247. https://doi.org/10.1016/j.icheatmasstransfer.2015.09.003
[41] Gad-el-Hak, M. "The Fluid Mechanics of Microdevices—The Freeman Scholar Lecture." *Journal of Fluids Engineering* 121, no. 1 (1999): 5-33. https://doi.org/10.1115/1.2822013
[42] Bahiraei, M., Heshmatian, S., and Keshavarzi, M. "Multi-attribute optimization of a novel micro liquid block working with green graphene nanofluid regarding preferences of decision maker." *Applied Thermal Engineering* 143 (2018): 11-21. https://doi.org/10.1016/j.applthermaleng.2018.07.074
[43] Arani, A.A.A., Akbari, O.A., Safaei, M.R., Marzban, A., Alrashed, A.A.A.A., Ahmadi, G.R., and Nguyen, T.K. "Heat transfer improvement of water/single-wall carbon nanotubes (SWCNT) nanofluid in a novel design of a truncated double-layered microchannel heat sink." *International Journal of Heat and Mass Transfer* 113 (2017): 780-795. https://doi.org/10.1016/j.ijheatmasstransfer.2017.05.089
[44] Nimmagadda, R., and Venkatasubbaiah, K. "Two-Phase Analysis on the Conjugate Heat Transfer Performance of Microchannel With Cu, Al, SWCNT, and Hybrid Nanofluids." *Journal of Thermal Science and Engineering Applications* 9, no. 4 (2017): 041011. https://doi.org/10.1115/1.4036804
[45] Bahiraei, M., Jamshidmofid, M., Amani, M., and Barzegarian, R. "Investigating exergy destruction and entropy generation for flow of a new nanofluid containing graphene–silver nanocomposite in a micro heat exchanger considering viscous dissipation." *Powder Technology* 336 (2018): 298-310. https://doi.org/10.1016/j.powtec.2018.06.007
[46] Bahiraei, M., and Heshmatian, S. "Thermal performance and second law characteristics of two new microchannel heat sinks operated with hybrid nanofluid containing graphene–silver nanoparticles." *Energy Conversion and Management* 168 (2018): 357-370. https://doi.org/10.1016/j.enconman.2018.05.020
[47] Ebrahimi, S., Sabbaghzadeh, J., Lajevardi, M., and Hadi, I. "Cooling performance of a microchannel heat sink with nanofluids containing cylindrical nanoparticles (carbon nanotubes)." *Heat and Mass Transfer* 46, no. 5 (2010): 549-553. https://doi.org/10.1007/s00231-010-0599-1
[48] Bergman, T.L., Lavine, A.S., Incropera, F.P., and DeWitt, D.P., *Fundamentals of Heat and Mass Transfer*. 8 ed. 2018: Wiley.
[49] Selvam, C., Mohan Lal, D., and Harish, S. "Thermal conductivity and specific heat capacity of water–ethylene glycol mixture-based nanofluids with graphene nanoplatelets." *Journal of Thermal Analysis and Calorimetry* 129, no. 2 (2017): 947-955. https://doi.org/10.1007/s10973-017-6276-6
[50] Sarsam, W.S., Amiri, A., Zubir, M.N.M., Yarmand, H., Kazi, S.N., and Badarudin, A. "Stability and thermophysical properties of water-based nanofluids containing triethanolamine-treated graphene nanoplatelets with different

specific surface areas." *Colloids and Surfaces A: Physicochemical and Engineering Aspects* 500 (2016): 17-31. https://doi.org/10.1016/j.colsurfa.2016.04.016

[51] Sadeghinezhad, E., Mehrali, M., Saidur, R., Mehrali, M., Tahan Latibari, S., Akhiani, A.R., and Metselaar, H.S.C. "A comprehensive review on graphene nanofluids: Recent research, development and applications." *Energy Conversion and Management* 111 (2016): 466-487. https://doi.org/10.1016/j.enconman.2016.01.004

[52] Sen Gupta, S., Manoj Siva, V., Krishnan, S., Sreeprasad, T.S., Singh, P.K., Pradeep, T., and Das, S.K. "Thermal conductivity enhancement of nanofluids containing graphene nanosheets." *Journal of Applied Physics* 110, no. 8 (2011): 084302. https://doi.org/10.1063/1.3650456

[53] Ting, T.W., Hung, Y.M., and Guo, N. "Field-synergy analysis of viscous dissipative nanofluid flow in microchannels." *International Journal of Heat and Mass Transfer* 73 (2014): 483-491. https://doi.org/10.1016/j.ijheatmasstransfer.2014.02.041

[54] Hung, Y.M. "Analytical Study on Forced Convection of Nanofluids With Viscous Dissipation in Microchannels." *Heat Transfer Engineering* 31, no. 14 (2010): 1184-1192. https://doi.org/10.1080/01457631003689344

[55] Shi, X., Li, S., Wei, Y., and Gao, J. "Numerical investigation of laminar convective heat transfer and pressure drop of water-based Al2O3 nanofluids in a microchannel." *International Communications in Heat and Mass Transfer* 90 (2018): 111-120. https://doi.org/10.1016/j.icheatmasstransfer.2017.11.007

[56] Ting, T.W., Hung, Y.M., and Guo, N. "Entropy generation of viscous dissipative nanofluid flow in thermal non-equilibrium porous media embedded in microchannels." *International Journal of Heat and Mass Transfer* 81 (2015): 862-877. https://doi.org/10.1016/j.ijheatmasstransfer.2014.11.006

[57] Sadaghiani, A.K., Yildiz, M., and Koşar, A. "Numerical modeling of convective heat transfer of thermally developing nanofluid flows in a horizontal microtube." *International Journal of Thermal Sciences* 109 (2016): 54-69. https://doi.org/10.1016/j.ijthermalsci.2016.05.022

[58] Anoop, K.B., Sundararajan, T., Das, S.K. "Effect of particle size on the convective heat transfer in nanofluid in the developing region." *International Journal of Heat and Mass Transfer* 52, no. 9 (2009): 2189-2195. https://doi.org/10.1016/j.ijheatmasstransfer.2007.11.063

[59] Akbarinia, A., and Laur, R. "Investigating the diameter of solid particles effects on a laminar nanofluid flow in a curved tube using a two phase approach." *International Journal of Heat and Fluid Flow* 30, no. 4 (2009): 706-714. https://doi.org/10.1016/j.ijheatfluidflow.2009.03.002

[60] Feng, Y., and Kleinstreuer, C. "Nanofluid convective heat transfer in a parallel-disk system." *International Journal of Heat and Mass Transfer* 53, no. 21 (2010): 4619-4628. https://doi.org/10.1016/j.ijheatmasstransfer.2010.06.031

[61] Ghasemi, S.E., Ranjbar, A.A., and Hosseini, M.J. "Experimental and numerical investigation of circular minichannel heat sinks with various hydraulic diameter for electronic cooling application." *Microelectronics Reliability* 73 (2017): 97-105. https://doi.org/10.1016/j.microrel.2017.04.028